

Integrative microscopy to explore physical and nanomechanical properties of eggshells of diapausing embryos in Rotifera: a proof-of-concept study

Stephanie Meyer, Thiago Q. Araujo, Elizabeth J. Walsh, Robert L. Wallace & Rick Hochberg

To cite this article: Stephanie Meyer, Thiago Q. Araujo, Elizabeth J. Walsh, Robert L. Wallace & Rick Hochberg (2023) Integrative microscopy to explore physical and nanomechanical properties of eggshells of diapausing embryos in Rotifera: a proof-of-concept study, *Journal of Natural History*, 57:45-48, 1984-2005, DOI: [10.1080/00222933.2023.2279255](https://doi.org/10.1080/00222933.2023.2279255)

To link to this article: <https://doi.org/10.1080/00222933.2023.2279255>



Published online: 05 Dec 2023.



Submit your article to this journal



View related articles



CrossMark

View Crossmark data



Integrative microscopy to explore physical and nanomechanical properties of eggshells of diapausing embryos in Rotifera: a proof-of-concept study

Stephanie Meyer ^a, Thiago Q. Araujo  ^a, Elizabeth J. Walsh  ^b, Robert L. Wallace  ^c and Rick Hochberg  ^a

^aDepartment of Biology, University of Massachusetts Lowell, Lowell, MA, USA; ^bDepartment of Biological Sciences, University of Texas, El Paso, TX, USA; ^cDepartment of Biology, Ripon College, Ripon, WI, USA

ABSTRACT

Diapausing embryos of invertebrates represent investments in future populations. Thus, they must be capable of withstanding a variety of environmental assaults. Consequently, their eggshells should be adapted to resist injuries from predators, sediments, or excessive shrinkage if desiccated. To date, there have been no direct nanomechanical measurements of the eggshells of most invertebrates that produce diapausing eggs. Here, we used three approaches to understand how the eggshells of two rotifers, a freshwater species (*Brachionus calyciflorus*) and a brackish-water species (*B. plicatilis*), tolerate harsh conditions: (1) atomic force microscopy to measure elasticity and hardness; (2) transmission electron microscopy to study ultrastructure; (3) scanning electron microscopy to examine surface features. We compared these values to measurements of brine shrimp (*Artemia salina*) cysts and mosquito (*Aedes aegypti*) overwintering eggs. Our results revealed that rotifer eggshells are structurally similar and have comparable nanomechanical values. While rotifer eggshells had lower Young's moduli (ca 13–16 MPa) and hardness values ($1.84\text{--}1.85 \times 10^{-2}$ GPa) than eggshells of *Artemia* and *Aedes*, eggshells of all species were relatively elastic and not particularly resistant to deformation. Pliancy of shells that form egg banks (ie *Artemia*, *Brachionus*) may be an adaptation to resist cracking under the physical forces associated with burial in sediments. Although there are no obvious relationships among eggshell thickness, ultrastructure, ornamentation, or nanomechanical values in rotifer eggshells, we hypothesise that eggshell composition may play an important role in determining elasticity and hardness. Future studies should consider an integrative approach to understand the importance of eggshell structure, chemistry, and mechanics in protecting diapausing embryos.

ARTICLE HISTORY

Received 4 July 2023
Accepted 30 October 2023

KEYWORDS

atomic force microscopy;
egg; mechanics;
zooplankton; diapause

Introduction

Both cladocerans and rotifers reproduce by cyclical parthenogenesis, a life-cycle strategy of facultative sexuality. In this strategy a population reproduces asexually via parthenogenesis, but the asexual sequence is periodically disrupted by bouts of sexuality (Cáceres

CONTACT Rick Hochberg  Rick_hochberg@uml.edu

© 2023 Informa UK Limited, trading as Taylor & Francis Group



and Tessier 2004; Serra *et al.* 2004; Kaupinis *et al.* 2017; García-Roger *et al.* 2019). Sexual reproduction results in the production of embryos that sink the bottom, residing in the sediments in a temporary state of suspended development (diapause) (Gilbert 1974, 2017). These embryos are encased in a specialised shell that can remain viable for long periods of time, thereby providing an egg bank for future populations (Carvalho and Wolf 1989; Hairston 1996; García-Roger *et al.* 2019; Vargas *et al.* 2019). Initiation of the switch to sexual reproduction usually depends on exogenous environmental factors, which generally include crowding, diet and photoperiod (Gilbert 2003; Koch *et al.* 2009, 2019), but in some populations endogenous factors may also play a role (Schröder *et al.* 2007). Production of diapausing embryos is considered to be a strategy to avoid impending adverse environmental conditions such as poor food supplies (Koch *et al.* 2009), predators (Ślusarczyk 1995), competitors (Aránguiz-Acuña and Ramos-Jiliberto 2014), or drying of the habitat (Schröder *et al.* 2007).

Ability to enter into embryonic dormancy has evolved numerous times in taxa with aquatic stages, and cyclical parthenogenesis is not a requirement for dormancy. For example, freshwater gastrotrichs produce both asexual and sexual diapausing embryos (Hummon 1984) and bryozoans produce asexual, non-embryonic statoblasts (Hengherr and Schill 2011). The metabolism of diapause apparently involves down- and up-regulation of specific pathways, cell cycle arrest, and production of metabolites that confer protection from environmental stress (García-Roger *et al.* 2019; Zhang *et al.* 2019; Huynh *et al.* 2021; Jia *et al.* 2022). Accordingly, significant efforts to understand the cellular, transcriptomic, and proteomic changes that occur as embryos enter and exit dormancy have been undertaken by several researchers (Hanson *et al.* 2013; Kaupinis *et al.* 2017; Ziv *et al.* 2017; Chen *et al.* 2018). So while we know something of the metabolism of diapause in some invertebrates, we have relatively little information on the protective capsules that shield them. This is particularly true for many freshwater microinvertebrates such as rotifers (Gilbert and Wurdak 1978; Wurdak *et al.* 1978) and cladocerans (Seidman and Larsen 1979; Kawasaki *et al.* 2004a, 2004b). While dormant in the sediment, diapausing embryos may be inhibited from hatching due to factors such as low light, oxygen and temperature (Gilbert 2017). They also may be subject to loss due to both biotic [egg-specific predation (Belmonte *et al.* 1997; Dumont *et al.* 2002; Waterkeyn *et al.* 2011) or deposit feeders (Albertsson and Leonardsson 2000, 2001)] and abiotic [low oxygen tension (Broman *et al.* 2015), hydrogen sulphide concentration (Sichlau *et al.* 2010), bioturbation (Viitasalo *et al.* 2007), and perhaps mechanical damage due to sediment compaction (García-Roger *et al.* 2005)] factors. The protective capsules of invertebrates, which are often referred to as cysts, resting eggs, or diapausing embryos, depending on the taxon, may provide a layer of protection that differs from those that protect asexual embryos. In monogonont rotifers, the eggshells of diapausing embryos differ from their amictic (subitaneous, tachyblastic) counterparts generally through increased thickness, addition of extra eggshell layers (or sublayers), and presence of ornamentation on the surface (Pourriot and Snell 1983; Schröder 2005).

To date, the eggshells of only three species of rotifers have been examined at the ultrastructural level: *Brachionus calyciflorus* Pallas, 1776, *Brachionus plicatilis* Müller, 1786, and *Asplanchna sieboldii* (Leydig, 1854) (Gilbert and Wurdak 1978; Wurdak *et al.* 1978; Munuswamy *et al.* 1996). Studies of these species reveal differences in surface features and ultrastructure of the eggshells. However, we know little of how ultrastructural

characteristics and nanomechanical properties may increase their probability of surviving diapause.

With this background, we posited that eggshells from species inhabiting different habitats will exhibit different ultrastructural characteristics and nanomechanical properties. To test these ideas, we examined eggshell characteristics of two species of *Brachionus* from habitats having different edaphic salt conditions: (1) *B. calyciflorus* is a common freshwater rotifer and (2) *B. plicatilis* is frequently present in coastal brackish ponds. For comparative purposes, we also examined two non-rotifer taxa whose embryos are capable of extended diapause: (1) cysts of the saline crustacean *Artemia salina* (Linnaeus, 1762) [hereafter *Artemia*], a well-known aquatic, parthenogenetic arthropod; and (2) *Aedes aegypti* (Linnaeus in Hasselquist, 1762) [hereafter *Aedes*], a freshwater insect that produces overwintering eggs. Both arthropods, and some rotifers, are known to have diapause eggshells that contain chitin (Morris and Afzelius 1967; Piavaux and Magis 1970; Sugumar and Munuswamy 2006), which is assumed to be a major factor in determining the stiffness (low elasticity, high hardness) of a biological material (Hou *et al.* 2021). However, the region assumed to contain chitin in rotifer eggshells is very thin; thus, whether chitin imparts a strong mechanical component to their eggshells remains unknown.

To determine whether there is a relationship between structure and nanomechanical properties, we applied three methods: scanning electron microscopy (SEM), transmission electron microscopy (TEM), and atomic force microscopy (AFM) (Krieg *et al.* 2018). The first two imaging techniques provide a wealth of data on structure, but they do not provide information on the nanomechanical properties of eggshells that can be useful in determining environmental resistance. AFM provides information on three attributes of surfaces: (1) surface topology, (2) elasticity and (3) hardness. Thus, our aim in using AFM was to determine whether it provides reliable data on topography that would supplement information provided by SEM, as well as providing data on the elasticity and hardness of the eggshells that can only be inferred from TEM data.

In this context we tested three main hypotheses. (1) Eggshells of rotifers will be more elastic than those of arthropods. This hypothesis is based on the presumption that *Brachionus* diapausing eggshells have less chitin than do the shells of *Artemia* and *Aedes*. (2) Eggshells of species of *Brachionus* and *Artemia* will be more elastic than *Aedes* eggshells. This hypothesis is based on the requirement of their eggshells having to withstand burial in the sediments, where they form egg banks: pliant eggshells should be less prone to cracking and exposing the embryo to the surrounding environment. Alternatively, mosquito eggs float on the surface of the water and do not form egg banks in the sediments. (3) Eggshells of *B. plicatilis* will be more resistant to deformation, ie harder, than the eggshells of *B. calyciflorus*. While both form egg banks within the sediments, and so must resist the forces exerted by the physical environment, the eggshells of the brackish-water species must also contend with more diverse predators. Salinity is an important regulator of benthic meiofauna diversity, and saline systems tend to have more diverse animals that may function as predators (Broman *et al.* 2019); hence, marine eggshells may be better adapted to resist mechanical degradation by predatory invertebrates.



Materials and methods

Specimens

Diapausing embryos of *Brachionus* were obtained in dehydrated form from commercial cultures at Sustainable Aquatics[©] (www.sustainableaquatics.com). Those of the freshwater species *B. calyciflorus* (Bc GAINES) were originally collected from the Gainesville, Florida strain. Diapausing embryos of the brackish/marine species *B. plicatilis* (Bp AUPEA006) were originally collected from a coastal brackish pond in Pearse Lakes, Australia. Cysts of *A. salina* were obtained from Carolina Biological Supply[©] (Burlington, NC, USA). Overwintering eggs of *A. aegypti* (USDA 'Gainesville' strain) were obtained from Benzon Research, Inc.[©] (Carlisle, PA, USA). Eggs used for AFM and SEM were placed in a desiccator for one week prior to study.

Electron microscopy

Eggs prepared for SEM were not preserved because we wanted to approximate how they would look when visualised with AFM (below). Eggs were mounted directly onto SEM stubs coated with carbon tape and then sputter coated with gold in a Denton Vacuum Desk IV prior to imaging with a JEOL JSM 6390 SEM at 15 kV at the University of Massachusetts Lowell. Using the SEM we measured the diameters of 10 specimens, recording their mean values, \pm 1 standard deviation (SD). For transmission electron microscopy (TEM), eggs were submersed directly in 2.5% glutaraldehyde in 0.1 M sodium cacodylate buffer for > 24 h. Eggs were subsequently rinsed (15 min \times 4) in 0.1 M sodium cacodylate buffer (with sucrose) and postfixed in 1% OsO₄ in 0.1 M sodium cacodylate buffer for 1 h prior to a second rinse in 0.1 M sodium cacodylate buffer (15 \times 4 min). Eggs were then transferred through an ethanol series (50%, 70%, 95%) for 20 min each followed by 100% (\times 2) at 30 min each. Eggs were then transferred through 3:1 ethanol: Spurr's low viscosity resin for 6 h, 1:1 overnight (minimum 16 h on a rotator), and then into a 1:3 ratio solution for 2 h. Eggs were placed in pure resin for 2 h and then transferred to pure resin in Better Equipment for Electron Microscopy (BEEM) capsules in an oven at 60°C for 18 h. Blocks were trimmed, sectioned with a glass knife on an ultramicrotome, and placed on gold grids. Grids were stained with uranyl acetate and lead citrate for 2 min each and examined on a Philips CM10 TEM (100 kV) at the University of Massachusetts Chan Medical School in Worcester, MA. Digital photos were obtained using a Gatan Ametek[®] digital camera. No manipulations to photos were made other than cropping and minor changes to brightness and contrast. Image J[©] (Schneider *et al.* 2012) was used to make measurements ($n = 10$) of shell thickness. In the case of *A. aegypti* eggs, where shell thickness values could not be determined from several publications, we made our own measurements using ImageJ[©] analysis of figures in Mundim-Pombo *et al.* (2021).

Atomic force microscopy

We separated out individual eggs from their plastic containers to ensure proper measurements and easy adherence to a flat silicon (Si) wafer. Because eggs often formed clumps, and collection of individual eggs with a fine tool can cause damage, we chose an ethanol-

water mixture as a form of 'benign' dispersant suspension medium following the protocol of other studies that required dispersing fine particles (McNamee *et al.* 2006). Other studies that have also performed AFM on microscopic animals (eg *Daphnia*: Rabus *et al.* 2013; rotifers: Yin *et al.* 2017) used ethanol as their medium of preservation, not as a dispersant. As the suspension of rotifer eggs dried on the Si wafer, the eggs formed a thin, single layer across the surface and could be measured one at a time without detaching them from the wafer. When dried, the samples were then imaged and measured on a Park XE-100 AFM at the University of Massachusetts Lowell. An NSC36 cantilever (Park Systems©: Korea) with a spring constant (k value) of 0.6 N/m was recommended by the manufacturer based on sample size and characteristics, and to minimise the risk of scratching the sample surface. For each species, five separate measurements per eggshell ($\times 2$ eggshells) were taken in randomly selected locations to generate an average. Multiple data points were needed due to variability in egg shape and topography. The use of five measurements was based on the study of Yin *et al.* (2017), where two adult rotifers were measured in five randomly selected areas to generate measurements of the lorica.

Park Systems XEI software (v. 5.2.4) was used to calculate the Young's modulus of elasticity (ratio of stress to strain) for each of five positions on two diapausing embryos. The Hertz model was selected as the contact mechanics model. Each position on the egg generates a force-distance curve: cursors need to be placed at the position of maximum force (green circle) and 20% maximum force (orange circle) from the baseline (eg see Figures 1f, 2f, 3d, 4d). A Poisson's ratio of 0.5 was entered to calculate Young's modulus, as recommended by the manufacturer; this value is standard for biological samples (Vinckier and Semenza 1998; Kontomaris and Malamou 2020).

To obtain a value for hardness (resistance to plastic deformation), equations from the Oliver and Pharr methodology were used (Oliver and Pharr 2004; Anon 2023). The hardness of a sample (H) is given by the equation 1:

$$H = \frac{F_{max}}{A}, \quad (1)$$

where F_{max} is the maximum force exerted on a sample in Newtons and A (m^2) is the contact area which is dependent on the tip geometry. F_{max} is obtained via the force-distance curve using the XEI software. The contact area (A) of the conical tip and sample is given by equation 2:

$$A = \pi \times \tan^2(\alpha) \times h_c^2, \quad (2)$$

where h_c is deformation of the sample and α is the half-angle of the conical tip. Deformation is obtained via the force-distance curve and α is given by the cantilever probe specification sheet provided by the manufacturer.

Measurements of Young's modulus and calculations of hardness for each of 10 locations on the diapausing embryos/cysts/overwintering eggs were made (Tables 1, 2).

Results

Below, we present the results by species and then technique. Because eggs from all species studied have been relatively well described at the ultrastructural level, we refrain from repeating detailed TEM observations and instead only focus on thickness and

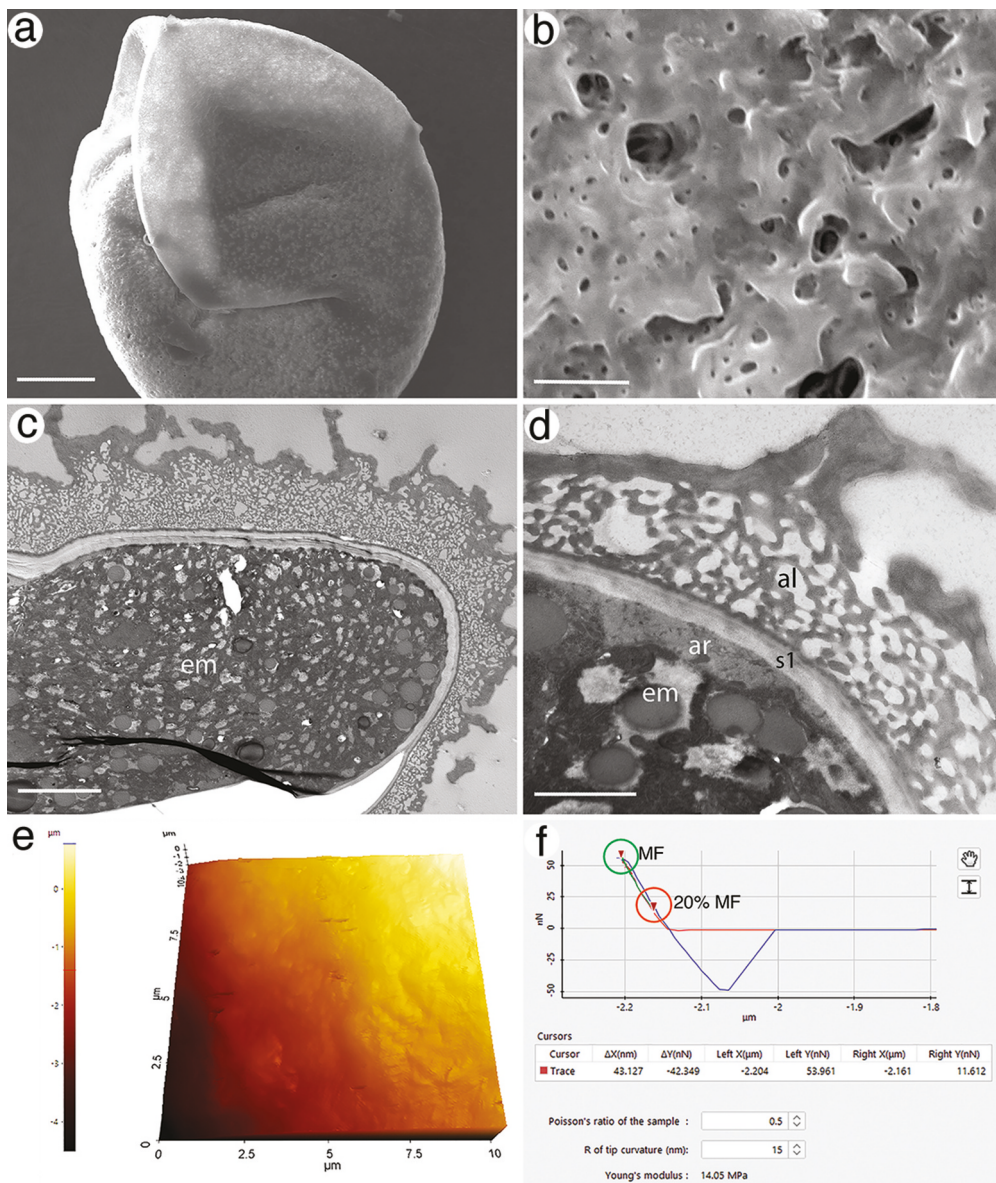


Figure 1. Characterisation of diapausing embryos of *Brachionus calyciflorus*. a. Scanning Electron Microscope image of a single egg. b. Close-up of the surface of the egg. c. Ultrastructure of the shell viewed with Transmission Electron Microscopy. d. Close-up of shell ultrastructure. e. Topographic image of the external surface of an egg generated with Atomic Force Microscopy. f. Force–distance (FD) curve generated from a single location on an egg. Parameters for the position of the location on the eggshell are indicated by the cursor positions (software screenshot). Maximum force (MF, green circle) and 20% maximum force (20% MF, orange circle) are indicated on the FD curve. Abbreviations: al, alveolar layer; ar, amorphous layer around embryo; em, embryo; s1, sublayer. Scale bars: A = 25 μm ; B = 5 μm ; C = 3.5 μm ; D = 1.7 μm .

Table 1. Young's modulus (MPa) of elasticity values for diapausing embryos of *Brachionus calyciflorus* and *Brachionus plicatilis*, cysts of *Artemia salina*, and overwintering eggs of *Aedes aegypti* measured in this study. Each column represents measurements on two eggs (five measurements per egg).

Rotifera		Arthropoda	
<i>B. calyciflorus</i>	<i>B. plicatilis</i>	<i>A. salina</i>	<i>A. aegypti</i>
14.23	12.24	21.17	21.40
9.73	13.88	21.11	26.88
16.83	16.62	22.51	21.01
12.62	15.18	21.96	16.69
14.46	15.11	22.42	14.09
13.88	17.19	22.27	28.61
10.54	15.96	17.40	24.83
17.21	12.93	19.96	24.78
12.14	19.15	20.44	28.46
14.51	19.85	20.07	18.62
Average Young's modulus (MPa)			
13.62	15.81	10.93	22.54
Standard deviation (MPa)			
2.43	2.49	1.57	5.01

Table 2. Hardness values ($\text{GPa} \times 10^{-2}$) for diapausing embryos of *Brachionus calyciflorus* and *Brachionus plicatilis*, cysts of *Artemia salina*, and overwintering eggs of *Aedes aegypti* measured in this study. Each column represents measurements on two eggs (five measurements per egg).

Rotifera		Arthropoda	
<i>B. calyciflorus</i>	<i>B. plicatilis</i>	<i>A. salina</i>	<i>A. aegypti</i>
1.62	1.14	1.90	1.78
1.64	1.41	1.94	1.84
1.67	1.48	2.19	2.10
1.67	1.57	2.22	2.18
1.75	1.73	2.22	2.32
1.78	1.76	2.26	2.48
1.85	1.77	2.26	2.50
1.85	2.18	2.30	2.53
2.00	3.00	2.35	2.67
2.18	5.31	2.43	2.75
Average hardness GPa			
1.84	1.85	2.20	2.28
Standard deviation GPa			
0.18	1.23	0.17	3.33

ornamentation as they might pertain to understanding eggshell mechanics in rotifers. A more detailed analysis of eggshell ultrastructure of diapausing embryos in rotifers, which includes an interpretation of eggshell chemistry and a reinterpretation of eggshell layering, will be published at a later date.



Phylum Rotifera: Brachionus calyciflorus

SEM

The ovoid, diapausing embryos measured ca 139 μm in diameter ($\bar{x} = 138.4 \pm 5.8 \mu\text{m}$). Shells appeared largely devoid of ornamentation at lower magnifications (< 1000 \times), but showed a more rugose surface at higher magnifications (Figure 1a,b). Shells often appeared pitted with small pores and craters (0.07–2.96 μm diameter) and occasionally some surface bumps of various textures.

TEM

The shell consisted of two layers – a thick apical layer and a thin basal layer – that together averaged $7.20 \pm 1.45 \mu\text{m}$ (SD) thick (Figure 1c). The surface of the shell had a wavy appearance and consisted of high ridges and numerous small bumps and valleys. Immediately beneath this was a thick zone of empty pockets that were interconnected through a framework of electron-dense bridges; this layer is described by Wurdak *et al.* (1978) as the alveolar layer (al: Figure 1d). Immediately beneath the alveolar layer was a zone [s1: Wurdak *et al.* (1978)] of less opaque electron density that consisted of two subzones, each containing many fine laminae, and separated by an electron-dense line. An extraembryonic space of variable size separated the physical shell from an amorphous region (ar) that was proximal to the plasma membrane of the embryo.

AFM

Topography of the outer shell layer was similar to that viewed with SEM, but pores were less visible ($\bar{x} = 0.23 \mu\text{m}$ diameter) and surface bumps were less recognisable (Figure 1e). An example force–distance curve is provided (Figure 1f) that displays how Young's modulus values were collected for a single spot on one egg. The Young's modulus for two diapausing embryos ranged from 9.73 to 17.21 MPa with an average of $13.62 \pm 2.43 \mu\text{Pa}$ (SD) (Table 1). Hardness values ranged from 1.62×10^{-2} to 2.18×10^{-2} GPa with an average hardness of $1.80 \times 10^{-2} \text{ GPa} \pm 1.80 \times 10^{-3} \text{ GPa}$ (Table 2).

Phylum Rotifera: Brachionus plicatilis

SEM

Diapausing embryos were ovoid and measured ca 134 μm in diameter ($\bar{x} = 134.0 \pm 4.0 \mu\text{m}$). The outer surface was composed of numerous smooth ridges and wrinkles, creating an overall rough surface (Figure 2a,b).

TEM

The shell consisted of a thick apical layer and a thin basal layer. Average shell thickness was $2.30 \pm 0.22 \mu\text{m}$ (SD). The outer layer, termed the alveolar layer by Munuswamy *et al.* (1996), had a wavy texture (Figure 2c,d). Electron density was highest at the topmost and bottom portions of the alveolar layer, otherwise it had a similar electron density throughout its thickness and contained many 'empty' pockets that were interconnected through electron-dense bridges. The basal layer [s1 of Munuswamy

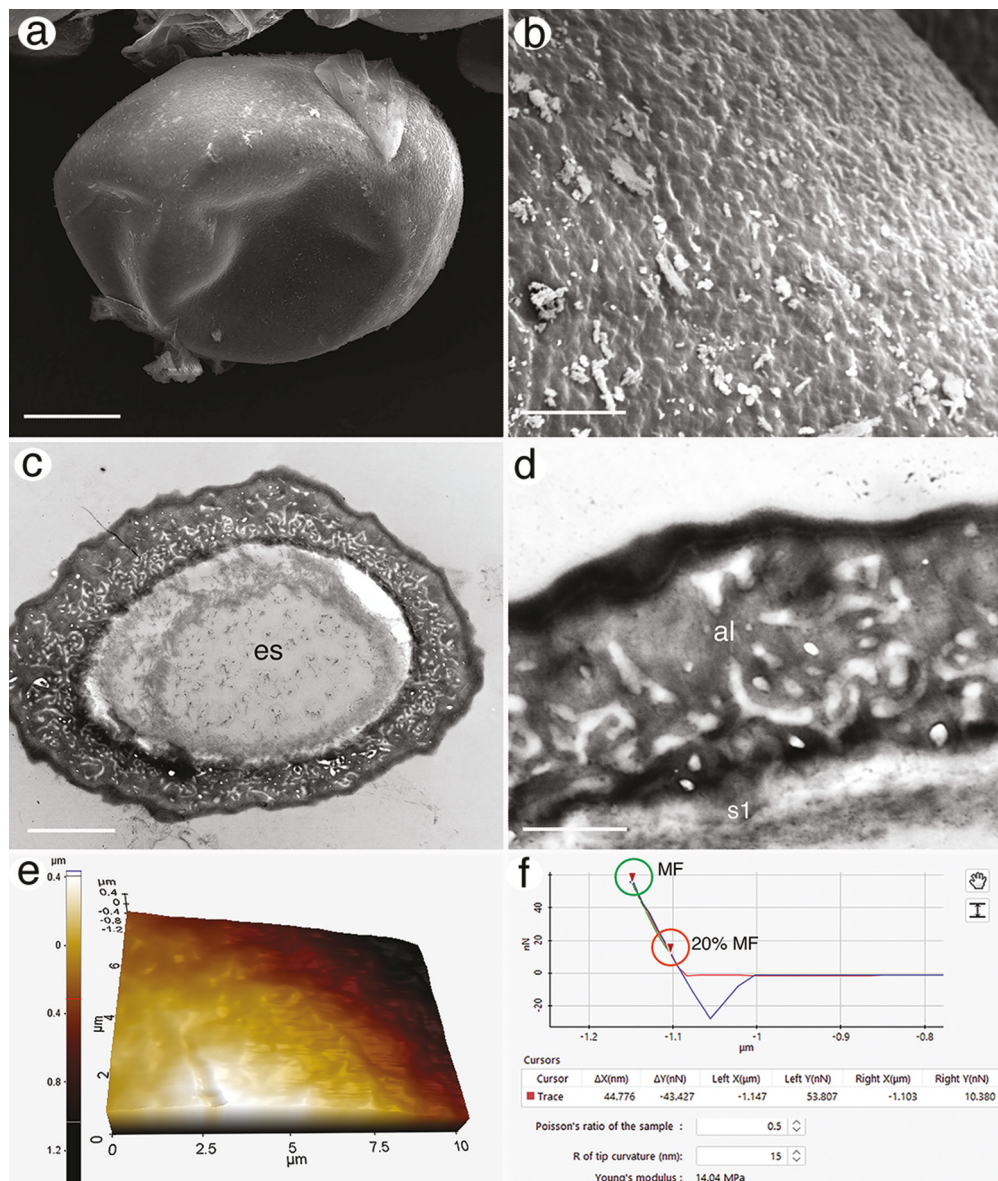


Figure 2. Characterisation of diapausing embryos of *Brachionus plicatilis*. a. Scanning Electron Microscope image of a single egg. b. Close-up of the surface of the egg. c. Ultrastructure of the shell viewed with Transmission Electron Microscopy. d. Close-up of shell ultrastructure. e. Topographic image of the external surface of an egg generated with Atomic Force Microscopy. f. Force–distance (FD) curve generated from a single location on an egg. Parameters for the position of the location on the eggshell are indicated by the cursor positions (software screenshot). Maximum force (MF, green circle) and 20% maximum force (20% MF, orange circle) are indicated on the FD curve. Abbreviations: al, alveolar layer; es, extraembryonic space (section did not include embryo); s1, sublayer. Scale bars: A = 25 μ m; B = 2 μ m; C = 6.5 μ m; D = 1.5 μ m.

et al. (1996)] had an amorphous appearance that consisted of an electron lucent zone and a more electron-opaque zone below it (Figure 2d). Thin fibres were present throughout both zones.

AFM

Topography of the outer shell showed rugosity and similar attributes to those in SEM, but with fewer details (Figure 2e). An example force–distance curve that displays how Young’s modulus values were collected for a single spot on one egg is shown in Figure 2f. The Young’s modulus ranged from 12.24 to 19.85 MPa with an average of 15.81 ± 2.49 MPa (SD) (Table 1). Hardness values ranged from 1.14×10^{-2} to 5.31×10^{-2} GPa with an average hardness of $1.853 \times 10^{-2} \pm 1.23 \times 10^{-2}$ GPa (Table 2).

Phylum Arthropoda: *Artemia salina*

SEM

The spherical egg (cyst) of *A. salina* measured ca 190 µm in diameter ($\bar{x} = 188.0 \pm 8.0$ µm). The smooth outer surface was devoid of any ornamentation but did show a small number of randomly distributed bumps and indentations (Figure 3a,b).

TEM

Not performed in this study. Measurements estimated from studies by Morris and Afzelius (1967), Mazzini (1978) and Sugumar and Munuswamy (2006) showed an average shell thickness of 7.50 ± 0.04 µm (SD).

AFM

Topography of the outer shell displayed comparable morphologies to those visualised with SEM, but with more texture observed under AFM (Figure 3c). Small bumps ranging in size from 0.3 to 1.1 µm were present on the surface. An example force–distance curve that displays how Young’s modulus values were collected for a single spot on one egg is shown in Figure 3d. The average Young’s modulus ranged from 17.40 to 22.51 MPa with a mean of 20.93 ± 1.57 MPa (SD) (Table 1). Hardness values ranged from 1.90×10^{-2} GPa to 2.43×10^{-2} GPa with a mean hardness of 2.20×10^{-2} GPa $\pm 1.67 \times 10^{-3}$ GPa (SD) (Table 2).

Phylum Arthropoda: *Aedes aegypti*

SEM

The elongate eggs of *A. aegypti* measured ca 600 µm long ($\bar{x} = 596.9 \pm 17.1$ µm). The posterior and anterior ends tapered into a spindle shape and the centre measured 165 µm in diameter (Figure 4a). The textured surface was covered with outer chorionic cells (*sensu* Mundim-Pombo *et al.* 2021). Each cell contained a central tubercle and smaller peripheral tubercles (Figure 4b). The central tubercles measured ca 7.6 µm in diameter and the peripheral tubercles measured ca 2.1 µm across. The surface of the shell was rugose in regions where tubercles and other ornamentation was absent (Figure 4c).

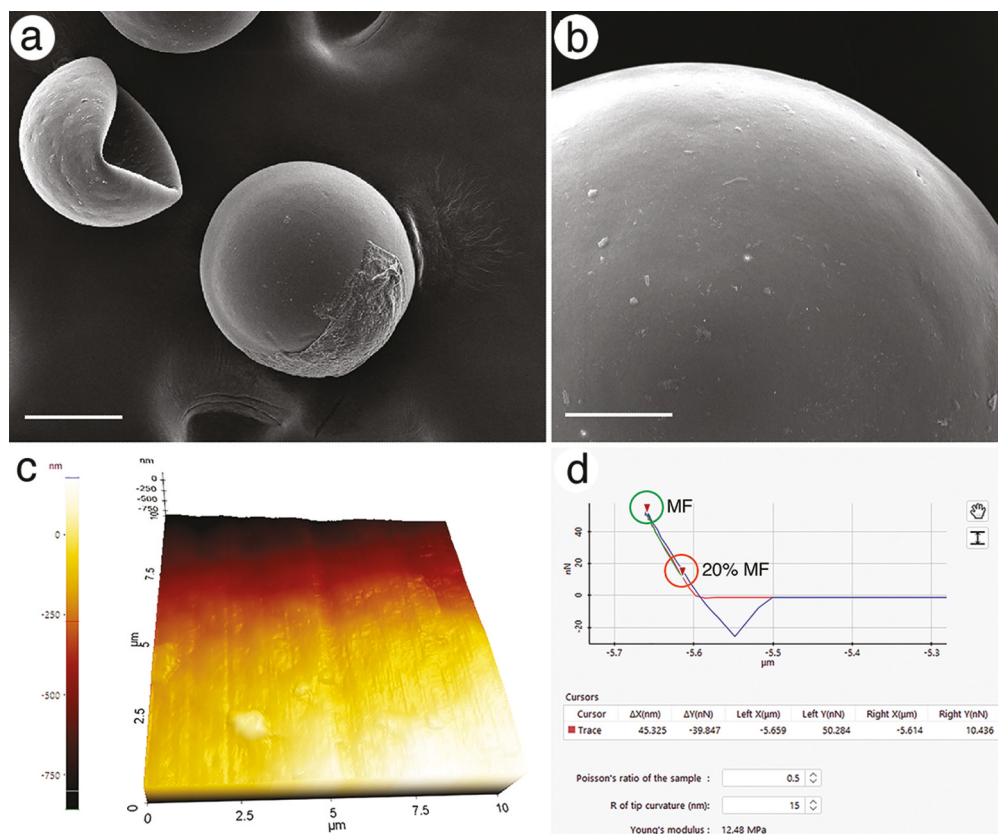


Figure 3. Characterisation of cysts of *Artemia salina*. a. Scanning Electron Microscopy of cysts. b. Close-up of the surface of a cyst. c. Topographic image of the external surface of a cyst generated with Atomic Force Microscopy. d. Force–distance (FD) curve generated from a single location on a cyst. Parameters for the position of the location on the eggshell are indicated by the cursor positions (screen shot). Maximum force (MF, green circle) and 20% maximum force (20% MF, orange circle) are indicated on the FD curve Scale bars: A = 100 μ m; B = 25 μ m.

TEM

Not performed in this study. Measurements estimated from Mundim-Pombo *et al.* (2021) showed an average shell thickness of 1.93 ± 0.63 μ m (SD).

AFM

Images of the outer shell layer displayed similar morphologies to those observed in SEM but were less textured. Small bumps on the eggshell measured ~ 0.79 μ m in diameter (Figure 4d). The AFM appeared to have taken measurements from the 'naked' region between tubercles or perhaps where tubercles were missing (probably artefactual and due to storage or processing) (see Figure 4a). An example force–distance curve that displays how Young's modulus values were collected for a single spot on one egg is shown in Figure 4e. The Young's modulus ranged from 14.09 to 28.61 MPa with an average of 22.54 ± 5.00 MPa (SD) (Table 1). The

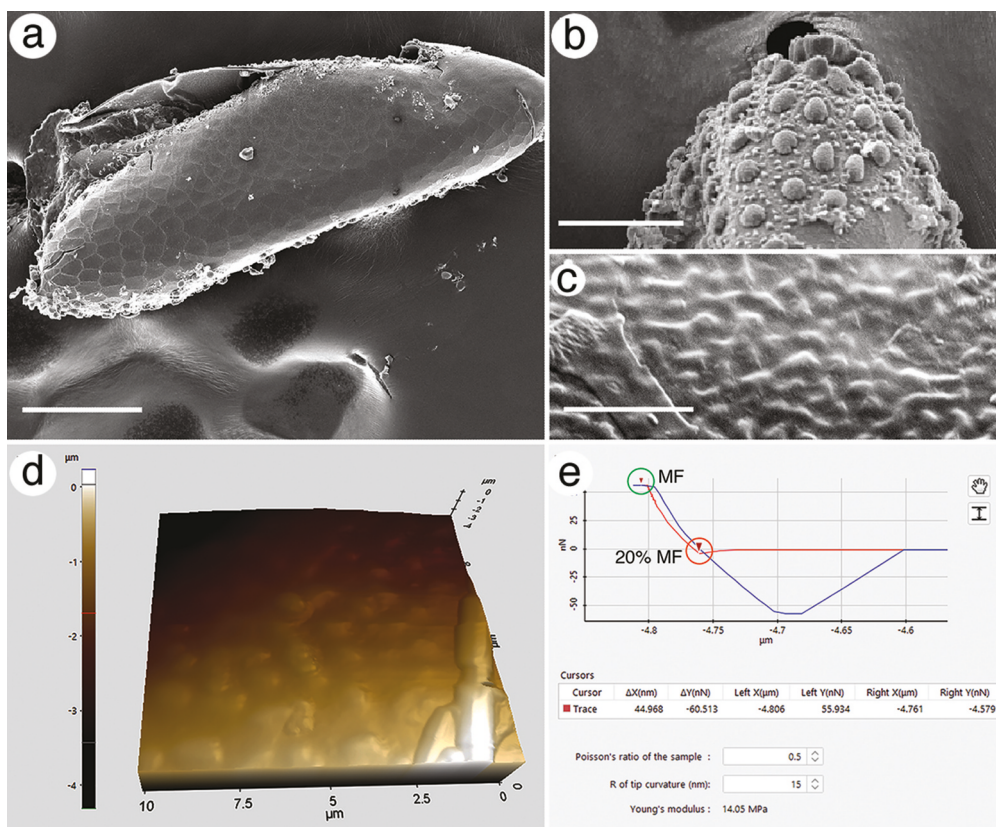


Figure 4. Characterisation of the overwintering eggs of *Aedes aegypti*. a. Scanning Electron Microscopy of an egg. The eggshell is damaged and much of the ornamentation has been artificially removed to expose the shell surface. b. Close-up of the ornamentation of an eggshell. c. Close-up of the surface of the eggshell region without ornamentation. d. Topographic image of the external surface of an eggshell generated with Atomic Force Microscopy. e. Force–distance (FD) curve generated from a single location on an eggshell. Parameters for the position of the location on the eggshell are indicated by the cursor positions (screen shot). Maximum force (MF, green circle) and 20% maximum force (20% MF, orange circle) are indicated on the FD curve. Scale bars: A = 100 μm; B = 53 μm; C = 15 μm.

hardness ranged from 1.78×10^{-2} GPa to 2.75×10^{-2} GPa with an average hardness of 2.28×10^{-2} GPa $\pm 3.33 \times 10^{-3}$ GPa (SD) (Table 2).

Discussion

This study attempted to determine whether analyses of eggshell structure using traditional electron microscopical methods could be supplemented by AFM, and whether there is a relationship between the physical structure of the eggshells and their nano-mechanical properties. We focused on brachionid rotifers because they are commercially available and the most well-studied rotifers (Dahms *et al.* 2011; Kostopoulou *et al.* 2012; Serra and Fontaneto 2017). Species of *Brachionus* are planktonic and occupy a variety of freshwater and saline regimes. In this study, we concentrated on two well-known species

from different habitats: *B. calyciflorus* from a freshwater pond and *B. plicatilis* from a coastal brackish pond. While both taxa comprise cryptic complexes (Gómez *et al.* 2002; Suatoni *et al.* 2006; Gabaldón *et al.* 2017; Mills *et al.* 2017), thereby complicating detailed species comparisons, their availability as verified monocultures from commercial supply companies lessens this concern. We also chose these species because their eggshells were previously studied with electron microscopy (Wurdak *et al.* 1978; Munuswamy *et al.* 1996). This allowed us to focus on the newly applied AFM methods and ensure that our nanomechanical data could be linked back to verified EM information rather than completely novel data. It also allows other researchers to perform similar studies on identical strains to determine whether our data can be verified using similar methods. We consider this research a proof-of-concept exercise that may provide valuable data to scientists who study diapause in rotifers and other microinvertebrates.

Species of *Brachionus* are the only rotifers that have been studied using AFM. Yin *et al.* (2017) used this technique to measure changes in the elasticity and hardness of the lorica (integument) of *Brachionus angularis* Gosse, 1851 and *B. calyciflorus* in response to kairomones of their predator, *Asplanchna brightwellii* Gosse, 1850. Their study relied on specimens preserved in ethanol (70%) to study the lorica, presumably because live animals are too difficult to stabilise under the AFM cantilever. Similarly, we chose to use an ethanol (50%) solution as a dispersant for the diapausing embryos so they could be easily sorted on a flat surface (Si wafer), stuck to it after drying, and studied individually; clumping would interfere with nanomechanical measurements. While effects of ethanol on the structural and nanomechanical properties of a rotifer's integument or its eggshells are unknown, we propose both of these studies may set a precedent for how future AFM studies of rotifers might proceed. With respect to studies on eggshells, we think these methods can be used to test hypotheses on how various physical characteristics of an eggshell such as ornamentation, thickness, layering, and presence of air pockets may affect a shell's resistance and dispersal capabilities.

Nanomechanics of diapausing eggshells

The nanomechanical properties of rotifer diapausing eggshells remain unknown despite their importance in counteracting environmental disturbance to the encapsulated embryo. In fact, few studies have used AFM or nanoindentation to study the mechanics of any invertebrate eggshells, whether in a diapause state or not. The only other study that attempted to understand the elasticity and hardness of an invertebrate's eggshell was that of Krenger *et al.* (2020), which applied microindentation to study the nematode *Caenorhabditis elegans* (Maupas, 1900). This species' eggshells are thin (300–400 nm: Krenger *et al.* 2020), well studied at the ultrastructural level (Bai *et al.* 2020; Bond and Huffman 2023), and consist of three layers: a thin vitelline layer, a thick middle layer, and a thin chondroitin proteoglycan layer. While Krenger *et al.* (2020) used a different form of microscopy to study nanomechanics – cellular force microscopy – it provided elasticity and hardness data similar to that generated with an AFM. Their study revealed a Young's modulus of elasticity (ratio of stress to strain) for the eggshell of 112 ± 26.2 (MPa). Importantly, elasticity is considered an intrinsic property of physical materials as it indicates the bond strength between atoms, ie a material with stronger bonds will have a higher modulus (be stiffer) than those with



weaker bonds (less stiff, more elastic). In the case of the nematode eggshell, Krenger *et al.* (2020) hypothesise that eggshell stiffness is best attributed to the chitin component, which is present in the thick middle layer, and so makes up the bulk of the eggshell. Studies have shown that when chitin is incorporated into a protein matrix such as that found in arthropod exoskeletons, the chitin molecules form covalent bonds with the proteins, and along with various side groups in the polymer matrix, as well as intra- and intermolecular hydrogen bonds, this makes chitinous materials tightly bonded (Hou *et al.* 2021) and highly resistant to degradation (Stankiewicz *et al.* 1998; Ofem *et al.* 2017; Hou *et al.* 2021). With respect to the nematode eggshell, when chitinase treatments were applied to the eggshells prior to measurement, the Young's modulus decreased to 6.5 ± 4.89 MPa, verifying the importance of chitin to eggshell stiffness.

The eggshells of diapausing embryos of rotifers are thicker (up to 7.20 μm in *B. calyciflorus*) than those of *C. elegans*, but are assumed to contain very little chitin, which is restricted to the 'most internal' envelope surrounding the embryo (Piavaux and Magis 1970). Unfortunately, no one has yet applied chitin labelling to the eggshells of diapausing rotifers; thus, the precise identity (eg position in the shell envelope and thickness of the chitin layer) in different rotifer eggshells is unknown. Wurdak *et al.* (1978) interpreted the chitinous region as a 40 nm membrane at the edge of a layer (edge of S2 of Wurdak *et al.* 1978), that in *B. calyciflorus* would be the electron-dense membrane separating the two laminated zones beneath the alveolar layer. If this is the case, and chitin is the major stiffening component of eggs, then this may explain the relatively low elastic modulus values of rotifer diapausing eggshells: approximately 13 MPa in *B. calyciflorus* and 16 MPa in *B. plicatilis*.

Our first hypothesis was that the eggshells of diapausing rotifer embryos would be more elastic (lower Young's modulus) than the eggshells of the two arthropods we studied. *Artemia salina* is a well-studied microcrustacean that forms resistant cysts with thick walls (Morris and Afzelius 1967; Sugumar and Munuswamy 2006). Some cyst layers contain chitin-binding domains (Ma *et al.* 2013), but chitin itself is mostly restricted to the fibrous layer of the embryonic cuticle that is several micrometres thick (Morris and Afzelius 1967; Sugumar and Munuswamy 2006). Curiously, our results show these cysts to have a relatively low elastic modulus (21 MPa), but this may have to do with the fact that our cantilever did not depress far enough into the eggshell to encounter the chitinous cuticle. Similarly, the overwintering eggs of *Aedes* have relatively low elastic moduli (~ 22 MPa), and although their shells are thicker than in the diapausing eggshell of rotifers, it is only the thin serosal cuticle that contains chitin (unmeasured by Farnesi *et al.* 2015). While our results verify the hypothesis that rotifer eggshells are more elastic than those of arthropods, the number of observations is too low to determine whether these results are significantly different.

Our second hypothesis was that species that form egg banks (*Artemia*, *Brachionus*) would have more pliant (elastic) eggshells than species with eggs that floated on the surface of the water (*Aedes*). Buried eggs should be adapted for the physical forces of the sediments around them (see below), and so pliancy (ie a low Young's modulus) will allow the shells to flex instead of breaking when contending with shallow or deep burial (see Snell *et al.* 1983 for a discussion of how burial depth may affect diapausing embryos and their eggshells). Our results do not confirm this hypothesis: the Young's moduli of

Brachionus, *Artemia* and *Aedes* eggshells were similar. It remains unknown why *Aedes* eggshells have such low Young's moduli, but without comparative data from the eggshells of other arthropods that oviposit on surface waters or in other environments, the question will remain an open one.

The Young's modulus of elasticity is generally considered proportional to hardness, which is defined as the measure of a material's ability to withstand localised permanent deformation (Labonte *et al.* 2017). Our third hypothesis was that the eggshells of the saline *B. plicatilis* would be harder than the eggshells of the freshwater *B. calyciflorus*. While both diapausing embryos form egg banks and need to resist the physical forces of the sediments (see below), we propose that the eggshells of diapausing embryos in marine sediments may be better adapted to resist predation by invertebrate predators like meiofauna, which tend to be more diverse and abundant in the sediments of more saline environments (Broman *et al.* 2015). A harder shell might therefore be more resistant to mechanical (but maybe not enzymatic?) destruction by predators. We calculated hardness values of freshwater and marine *Brachionus* eggshells to be similar ($\sim 1.80 \times 10^{-2}$ GPa), which argues against marine shells being harder than freshwater shells. Curiously, the hardness values of the eggshells were two orders of magnitude lower than the hardness values obtained on the integument of species of *Brachionus* (Yin *et al.* 2017) under natural conditions: 1.54 ± 0.08 GPa for *B. calyciflorus* and 3.28 ± 0.05 GPa for *B. angularis*. The rotifer lorica is much thinner than the eggshell envelopes of *B. calyciflorus* (117.95 ± 12.79 nm) and *B. angularis* (338.29 ± 0.05 nm), meaning that hardness is not proportional to the thickness of the material being tested. This suggests that rotifer eggshells are less resistant to deformation than the body walls of the adults that lay the eggs, and that something other than thickness is the cause for the low hardness values of eggshells of their diapausing embryos.

Adaptive significance of elasticity and hardness

What do low values of Young's modulus and hardness mean for eggshells in the sediment? This question remains difficult to answer without comparative studies and additional testing, but we attempt an interpretation based on studies of vertebrate eggshells, which have received more attention (Torres *et al.* 2010; Hincke *et al.* 2012; Chang and Chen 2016; Sellés *et al.* 2019). As an example, Chang and Chen (2016) studied the eggshells of two reptiles that bury their eggs: the Chinese striped-neck turtle *Mauremys (Ocadia) sinensis* (Gray, 1870) and the Taiwan cobra snake *Naja atra* Cantor, 1842. After decalcification to remove the mineral phase of the eggshells, which is necessary for mechanical testing, the turtle eggshells had a Young's modulus of 100–400 MPa, and the snake eggshells had a value of 10–15 MPa. Further examinations included histological staining, measurements of crack propagation, cyclic tests in tension, and penetration testing. Combined, these data revealed that snake eggshells are more flexible and tougher, and have higher extensibility (lower Young's modulus) than turtle eggshells; this is attributed to the wavy and random arrangement of unmineralised keratin and collagen fibres in the snake eggshells. In contrast, turtle eggshells have straight keratin fibres that are highly mineralised, which makes them stiffer and brittle (higher Young's modulus). Because the two species had similar keratin concentrations, the authors interpret keratin fibre arrangement as a major factor in determining the substrate resistance of reptile eggshells. Although such vertebrate eggshells and rotifer eggshells cannot be



directly compared due to their sizes and habitat differences, the reptile study does provide evidence that nanomechanical values are tied to physical and chemical factors of the shell that we have yet to investigate in rotifers.

We currently postulate that the eggshells of rotifer diapausing embryos have low values of Young's modulus and hardness as an adaptation to resist environmental factors after they settle into the sediment forming the egg bank (eg Gómez *et al.* 2000; García-Roger *et al.* 2006a, 2006b). Studies of diapausing embryo viability have shown a correlation between sediment depth and egg health, with deeper depths leading to physical deterioration (García-Roger *et al.* 2005). Substrate-related factors such as sediment age, contact forces (eg sorting, grain size), and gravity may be the primary agencies that led to eggshells evolving high elasticity and lacking resistance to permanent deformation, and while these factors are not the only forces that eggshells have to contend with (eg changes in water chemistry and oxygen), they may be the dominant factors that ultimately drove the evolution of eggshell stiffness. After all, rotifer diapausing embryos must first contend with the influence of physical factors in sediments prior to other factors that may hamper embryonic development, such as benthic predation pressure and potential desiccation (ie if the water body dries up).

Future considerations

Our study of the eggshells of two species of *Brachionus* provides proof that imaging and measurements can be made using AFM. What remains difficult to determine is if our measured values of Young's modulus and the calculations of hardness have been interpreted correctly in the context of the environment in which eggs are oviposited. Because no other studies have followed a similar protocol to ours, and indeed only one other study has measured a comparably sized invertebrate eggshell (Krenger *et al.* 2020), we hesitate to make assumptions about how eggshell ornamentation, thickness, and chemistry contribute to nanomechanical properties. Nevertheless, we think that studies of additional rotifer eggshells from a wider variety of species may provide the data necessary to properly interpret the nanomechanical properties of rotifer eggshells. As evidenced by the study of vertebrate eggshells, there are many methods that can be used to study nanomechanical properties, but whether such tests can be performed on microscopic eggs remains to be determined. At minimum, we think that future studies should combine AFM data, TEM data (structure, chemistry via heavy metal staining), and perhaps enzyme testing (eg chitinase, keratinases) over a wide range of species to determine whether there is a correlation between elasticity/hardness values and structure/chemistry.

If nanomechanical values can be obtained with some reliability across a range of species, then we think this will open an avenue for exploring how other factors such as maternal nutrition and other environment variables may influence eggshell properties and hence their ability to withstand the benthic environment as well as aerial dispersion (anemochory). We provide a brief list of topics below that we believe are worth exploring after AFM has become more standardised for measuring rotifer eggshells.

Parental effects

Martínez-Ruiz and García-Roger (2014) showed that rotifer diapause eggshells display intraspecific variation ('within-genotype variation') due to metabolic resources provided to offspring, which results in earlier eggs receiving more resources than later eggs, ie as a function

of laying order. Whether or not this explains the size variation in diapausing embryos within a species remains to be determined, but such variation has been noted across Rotifera (Nipkow 1958; Bogoslovsky 1963; Pourriot 1967; Snell *et al.* 1983). Regardless, a study of the eggshells from a single mother and/or clone on a consistent (standardised or experimental) diet may help to understand their effects on eggshell nanomechanical properties.

Environmental effects

Snell *et al.* (1983) hypothesised that diapause eggshell size variation (within a population or species) may be in part due to increases in osmotic pressure as eggs are buried deeper, ie smaller eggshells were found in deeper sediments. They postulate that the space between eggshell and embryo (extraembryonic space) may shrink in eggs at deeper depths, making eggshells effectively smaller, hence their pliancy is an adaptation to substrate-level forces. AFM and TEM studies of eggs collected at different depths may provide the evidence necessary to confirm this hypothesis.

Effects of desiccation

Diapausing embryos are resistant to desiccation, which is adaptive when water bodies dry up and/or are dispersed by anemochory (Rivas *et al.* 2018, 2019) or by animals (zoochory) (Moreno *et al.* 2019). We measured nanomechanical values of dry eggs; therefore, our study approximates the stresses that they would suffer when abraded by sand while buried or when entrained in dust transport, as is seen in arid lands (Rivas *et al.* 2018, 2019). Future studies might consider testing the elasticity and hardness of wet samples to determine whether the values differ from dry samples. Our AFM (Park XE-100) could not accommodate wet samples; however, other AFMs can measure the elastic properties of biological materials while immersed in fluid (Efremov *et al.* 2020). Such a comparative study would provide relevant insights into how eggshell properties change as they go through desiccation and rehydration across seasons.

Acknowledgements

This study is based on the Master's thesis of the first author and supported by NSF grants to the following individuals: R. Hochberg (DEB 2051684), R.L. Wallace (DEB 2051710), and E.J. Walsh (DEB 2051704). We thank Dr Earl Ada in the Materials Characterization Laboratory (UML) for his assistance with AFM, and the staff at the Electron Microscopy Facility at UMASS Chan Medical School in Worcester, MA, for their assistance. We also thank two anonymous reviewers for their comments and recommendations.

Author contributions

SM: data collection and interpretation; SM, RH: conduct of experiments, interpretation of data; SM, TQA, RW, EM, RH: writing of manuscript.

Disclosure statement

No potential conflict of interest was reported by the authors.

Funding

This work was supported by the National Science Foundation [DEB 2051684].

ORCID

Stephanie Meyer  <http://orcid.org/0009-0008-2832-349X>
 Thiago Q. Araujo  <http://orcid.org/0000-0001-9325-6248>
 Elizabeth J. Walsh  <http://orcid.org/0000-0002-6719-6883>
 Robert L. Wallace  <http://orcid.org/0000-0001-6305-4776>
 Rick Hochberg  <http://orcid.org/0000-0002-5567-5393>

References

Albertsson J, Leonardsson K. 2000. Impact of a burrowing deposit-feeder, *Monoporeia affinis*, on viable zooplankton resting eggs in the northern Baltic. *Mar Biol.* 136:611–619. doi: [10.1007/s002270050721](https://doi.org/10.1007/s002270050721).

Albertsson J, Leonardsson K. 2001. Deposit-feeding amphipods (*Monoporeia affinis*) reduce the recruitment of copepod nauplii from benthic resting eggs in the northern Baltic Sea. *Mar Biol.* 138:793–801. doi: [10.1007/s002270000498](https://doi.org/10.1007/s002270000498).

Anon. 2023. Nanoindentation training guide V1.1. Park Systems Corp; p. 77

Aránguiz-Acuña A, Ramos-Jiliberto R. 2014. Diapause may promote coexistence of zooplankton competitors. *J Plankton Res.* 36(4):978–988. doi: [10.1093/plankt/fbu034](https://doi.org/10.1093/plankt/fbu034).

Bai X, Huang LJ, Chen SW, Nebenfuehr B, Wysolmerski B, Wu JC, Olson SK, Golden A, Wang CW. 2020. Loss of the seipin gene perturbs eggshell formation in *Caenorhabditis elegans*. *Development.* 147: dev192997. doi: [10.1242/dev.192997](https://doi.org/10.1242/dev.192997).

Belmonte G, Miglietta A, Rubino F, Boer F. 1997. Morphological convergence of resting stages of planktonic organisms: a review. *Hydrobiologia.* 355:159–165. doi: [10.1023/A:1003071205424](https://doi.org/10.1023/A:1003071205424).

Bogoslovsky AS. 1963. Materials to the study of the resting eggs of rotifers. *Biulleten' Moskovskogo Obschestva Ispytatelei Prirody Otdel Biologicheskii.* 68:50–67. (In Russian with English summary; on *Brachionus calyciflorus*).

Bond AT, Huffman DG. 2023. Nematode eggshells: a new anatomical and terminological framework, with a critical review of relevant literature and suggested guidelines for the interpretation and reporting of eggshell imagery. *Parasite.* 30:6. doi: [10.1051/parasite/2023007](https://doi.org/10.1051/parasite/2023007).

Broman EM, Brüsén M, Dopson S, Hylander S. 2015. Oxygenation of anoxic sediments triggers hatching of zooplankton eggs. *P R Soc B.* 282(1817):20152025. doi: [10.1098/rspb.2015.2025](https://doi.org/10.1098/rspb.2015.2025).

Broman E, Raymond C, Sommer C, Gunnarsson JS, Creer S, Nascimento FJA. 2019. Salinity drives meiofaunal community structure dynamics across the Baltic ecosystem. *Mol Ecol.* 28 (16):3813–3829. doi: [10.1111/mec.15179](https://doi.org/10.1111/mec.15179).

Cáceres CE, Tessier AJ. 2004. Incidence of diapause varies among populations of *Daphnia pulicaria*. *Oecologia.* 141(3):425–431. doi: [10.1007/s00442-004-1657-5](https://doi.org/10.1007/s00442-004-1657-5).

Carvalho GR, Wolf HG. 1989. Resting eggs of lake-*Daphnia* I. Distribution, abundance and hatching of eggs collected from various depths in lake sediments. *Freshwater Biol.* 22(3):459–470. doi: [10.1111/j.1365-2427.1989.tb01118.x](https://doi.org/10.1111/j.1365-2427.1989.tb01118.x).

Chang Y, Chen P-Y. 2016. Hierarchical structure and mechanical properties of snake (*Naja atra*) and turtle (*Ocadia sinensis*) eggshells. *Acta Biomater.* 31:33–49. doi: [10.1016/j.actbio.2015.11.040](https://doi.org/10.1016/j.actbio.2015.11.040).

Chen L, Barnett RE, Horstmann M, Bamberger V, Heberle L, Krebs N, Colbourne JK, Gómez R, Weiss LC. 2018. Mitotic activity patterns and cytoskeletal changes throughout the progression of diapause developmental program in *Daphnia*. *BMC Cell Biol.* 19:1–12. doi: [10.1186/s12860-018-0181-0](https://doi.org/10.1186/s12860-018-0181-0).

Dahms H-U, Hagiwara A, Lee J-S. 2011. Ecotoxicology, ecophysiology, and mechanistic studies with rotifers. *Aquat Toxicol.* 101(1):1–12. doi: [10.1016/j.aquatox.2010.09.006](https://doi.org/10.1016/j.aquatox.2010.09.006).

Dumont HJ, Nandini S, Sarma SSS. 2002. Cyst ornamentation in aquatic invertebrates: a defence against egg-predation. *Hydrobiologia*. 486:161–167. doi: [10.1023/A:1021346601235](https://doi.org/10.1023/A:1021346601235).

Efremov YM, Bakhchieva NA, Shavkuta BS, Frolova AA, Kotova SL, Novikov IA, Akovantseva AA, Avetisov KA, Avetisov SE, Timashev PS. 2020. Mechanical properties of anterior lens capsule assessed with AFM and nanoindenter in relation to human aging, pseudoexfoliation syndrome, and trypan blue staining. *J Mech Beh Biomed Mat.* 112:104081. doi: [10.1016/j.jmbbm.2020.104081](https://doi.org/10.1016/j.jmbbm.2020.104081).

Farnesi LC, Menna-Barreto RF, Martins AJ, Valle D, Rezende GL. 2015. Physical features and chitin content of eggs from the mosquito vectors *Aedes aegypti*, *Anopheles aquasalis* and *Culex quinquefasciatus*: connection with distinct levels of resistance to desiccation. *J Insect Phys.* 83:43–52. doi: [10.1016/j.jinsphys.2015.10.006](https://doi.org/10.1016/j.jinsphys.2015.10.006).

Gabaldón C, Fontaneto D, Carmona MJ, Montero-Pau J, Serra M. 2017. Ecological differentiation in cryptic rotifer species: what we can learn from the *Brachionus plicatilis* complex. *Hydrobiologia*. 796(1):7–18. doi: [10.1007/s10750-016-2723-9](https://doi.org/10.1007/s10750-016-2723-9).

García-Roger EM, Carmona MJ, Serra M. 2005. Deterioration patterns in diapausing egg banks of *Brachionus* (Müller, 1786) rotifer species. *J Exp Mar Biol Ecol.* 314(2):149–161. doi: [10.1016/j.jembe.2004.08.023](https://doi.org/10.1016/j.jembe.2004.08.023).

García-Roger EM, Carmona MJ, Serra M. 2006a. Patterns in rotifer diapausing egg banks: density and viability. *J Exp Mar Biol Ecol.* 336:198–210. doi: [10.1016/j.jembe.2006.05.009](https://doi.org/10.1016/j.jembe.2006.05.009).

García-Roger EM, Carmona MJ, Serra M. 2006b. A simple model relating habitat features to a diapause egg bank. *Limnol Ocean.* 51(3):1542–1547. doi: [10.4319/lo.2006.51.3.1542](https://doi.org/10.4319/lo.2006.51.3.1542).

García-Roger EM, Lubzens E, Fontaneto D, Serra M. 2019. Facing adversity: dormant embryos in rotifers. *Biol Bull.* 237(2):119144. doi: [10.1086/705701](https://doi.org/10.1086/705701).

Gilbert JJ. 1974. Dormancy in rotifers. *Trans Am Microsc Soc.* 93(4):490–513. doi: [10.2307/3225154](https://doi.org/10.2307/3225154).

Gilbert JJ. 2003. Specificity of crowding response that induces sexuality in the rotifer *Brachionus*. *Limnol Oceangr.* 48(3):1297–1303. doi: [10.4319/lo.2003.48.3.1297](https://doi.org/10.4319/lo.2003.48.3.1297).

Gilbert JJ. 2017. Resting-egg hatching and early population development in rotifers: a review and a hypothesis for differences between shallow and deep waters. *Hydrobiologia*. 796(1):235–243. doi: [10.1007/s10750-016-2867-7](https://doi.org/10.1007/s10750-016-2867-7).

Gilbert JJ. 2019. Variation in the life cycle of monogonont rotifers: commitment to sex and emergence from diapause. *Freshwater Biol.* 65:786–810. doi: [10.1111/fwb.13440](https://doi.org/10.1111/fwb.13440).

Gilbert JJ, Wurdak ES. 1978. Species-specific morphology of resting eggs in the rotifer *Asplanchna*. *Trans Am Microsc Soc.* 97(3):330–339. doi: [10.2307/3225986](https://doi.org/10.2307/3225986).

Gómez A, Carvalho GR, Lunt DH. 2000. Phylogeography and regional endemism of a passively dispersing zooplankton: mitochondrial DNA variation in rotifer resting egg banks. *P R S London.* 267(1458):2189–2197. doi: [10.1098/rspb.2000.1268](https://doi.org/10.1098/rspb.2000.1268).

Gómez A, Serra M, Carvalho GR, Lunt DH. 2002. Speciation in ancient cryptic species complexes: evidence from the molecular phylogeny of *Brachionus plicatilis* (Rotifera). *Evolution.* 56 (7):1431–1444. doi: [10.1554/0014-3820\(2002\)056\[1431:SIACSC\]2.0.CO;2](https://doi.org/10.1554/0014-3820(2002)056[1431:SIACSC]2.0.CO;2).

Hirston NG Jr. 1996. Zooplankton egg banks as biotic reservoirs in changing environments. *Limnol Ocean.* 41(5):1087–1092. doi: [10.4319/lo.1996.41.5.1087](https://doi.org/10.4319/lo.1996.41.5.1087).

Hanson SJ, Stelzer CP, Mark Welch DB, Logsdon JM. 2013. Comparative transcriptome analysis of obligately asexual and cyclically sexual rotifers reveals genes with putative functions in sexual reproduction, dormancy, and asexual egg production. *BMC Genomics.* 14:1–17. doi: [10.1186/1471-2164-14-412](https://doi.org/10.1186/1471-2164-14-412).

Hengherr S, Schill RO. 2011. Dormant stages in freshwater bryozoans—an adaptation to transcend environmental constraints. *J Insect Phys.* 57(5):595–601. doi: [10.1016/j.jinsphys.2011.03.018](https://doi.org/10.1016/j.jinsphys.2011.03.018).

Hincke MT, Nys Y, Gautron J, Mann K, Rodriguez-Navarro AB, McKee MD. 2012. The eggshell: structure, composition and mineralization. *Front Biosci Landmark.* 17(4):1266–1280. doi: [10.2741/3985](https://doi.org/10.2741/3985).

Hou J, Aydemir BE, Dumanli AG. 2021. Understanding the structural diversity of chitins as a versatile biomaterial. *Philo T R Soc A.* 379:20200331. doi: [10.1098/rsta.2020.0331](https://doi.org/10.1098/rsta.2020.0331).

Hummon MR. 1984. Reproduction and sexual development in a freshwater gastrotrich. 1. Oogenesis of parthenogenetic eggs (Gastrotricha). *Zoomorphology.* 104:33–41. doi: [10.1007/BF00312169](https://doi.org/10.1007/BF00312169).

Huynh TV, Hall AS, Xu S. **2021**. The transcriptomic signature of cyclical parthenogenesis. *bioRxiv*. 2021:2021–2029.

Jia J, Dong C, Han M, Ma S, Chen W, Dou J, Feng C, Liu X. **2022**. Multi-omics perspective on studying reproductive biology in *Daphnia sinensis*. *Genomics*. 114(2):110309. doi: [10.1016/j.ygeno.2022.110309](https://doi.org/10.1016/j.ygeno.2022.110309).

Kaupinis A, Aitmanaitė L, Strepetkaitė D, Valius M, Lazutka JR, Arbačiauskas K. **2017**. Proteomic and gene expression differences between post-diapause and subitaneous offspring phenotypes in the cyclic parthenogen *Daphnia pulex*. *Hydrobiologia*. 798:87–103. doi: [10.1007/s10750-016-3057-3](https://doi.org/10.1007/s10750-016-3057-3).

Kawasaki T, Sakata M, Namiki H. **2004a**. Elemental characterization of *Daphnia* resting eggs by X-ray analytical microscopy. *Zool Sci*. 21:1019–1023. doi: [10.2108/zsj.21.1019](https://doi.org/10.2108/zsj.21.1019).

Kawasaki T, Yoshimura H, Shibue T, Ikeuchi Y, Sakata M, Garashi K, Takada H, Hoshino K, Kohn K, Namiki H. **2004b**. Crystalline calcium phosphate and magnetic mineral content of *Daphnia* resting eggs. *Zool Sci*. 21:63–67. doi: [10.2108/0289-0003\(2004\)21\[63:CCPAMM\]2.0.CO;2](https://doi.org/10.2108/0289-0003(2004)21[63:CCPAMM]2.0.CO;2).

Koch U, von Elert E, Straile D. **2009**. Food quality triggers the reproductive mode in the cyclical parthenogen *Daphnia* (Cladocera). *Oecologia*. 159(2):317–324. doi: [10.1007/s00442-008-1216-6](https://doi.org/10.1007/s00442-008-1216-6).

Kontomaris SV, Malamou A. **2020**. Hertz model or Oliver and Pharr analysis? Tutorial regarding AFM nanoindentation experiments on biological samples. *Mat Res Express*. 7(3):033001. doi: [10.1088/2053-1591/ab79ce](https://doi.org/10.1088/2053-1591/ab79ce).

Kostopoulou V, Carmona MJ, Divanach P. **2012**. The rotifer *Brachionus plicatilis*: an emerging bio-tool for numerous applications. *J Biol Res Thessaloniki*. 17:97–112.

Krenger R, Burri JT, Lehnert T, Nelson BJ, Gijs MAM. **2020**. Force microscopy of the *Caenorhabditis elegans* embryonic eggshell. *Microsyst Nanoeng*. 6:29. doi: [10.1038/s41378-020-0137-3](https://doi.org/10.1038/s41378-020-0137-3).

Krieg M, Fläschner G, Alsteens D, Gaub BM, Roos WH, Wuite GJL, Gaub HE, Gerber C, Dufrêne YF, Müller DJ. **2018**. Atomic force microscopy-based mechanobiology. *Nat Rev Phys*. 1(1):41–57. doi: [10.1038/s42254-018-0001-7](https://doi.org/10.1038/s42254-018-0001-7).

Labonte D, Lenz AK, Oyen ML. **2017**. On the relationship between indentation hardness and modulus, and the damage resistance of biological materials. *Acta Biomater*. 57:373–383. doi: [10.1016/j.actbio.2017.05.034](https://doi.org/10.1016/j.actbio.2017.05.034).

Ma WM, Li HW, Dai ZM, Yang JS, Yang F, Yang WJ. **2013**. Chitin-binding proteins of *Artemia* diapause cysts participate in formation of the embryonic cuticle layer of cyst shells. *Biochem J*. 449 (1):285–294. doi: [10.1042/BJ20121259](https://doi.org/10.1042/BJ20121259).

Martínez-Ruiz C, García-Roger EM. **2014**. Being first increases the probability of long diapause in rotifer resting eggs. *Hydrobiologia*. 745(1):111–121. doi: [10.1007/s10750-014-2098-8](https://doi.org/10.1007/s10750-014-2098-8).

Mazzini M. **1978**. Scanning electron microscope morphology and amino-acid analysis of the egg-shell of encysted brine shrimp, *Artemia salina* Leach (Crustacea Anostraca). *Monit Zool Ital*. 12(4):243–252. doi: [10.1080/00269786.1978.10736321](https://doi.org/10.1080/00269786.1978.10736321).

McNamee CE, Pyo N, Higashitani K. **2006**. Atomic force microscopy study of the specific adhesion between a colloid particle and a living melanoma cell: effect of the charge and the hydrophobicity of the particle surface. *Biophysical J*. 91:1960–1969. doi: [10.1529/biophysj.106.082420](https://doi.org/10.1529/biophysj.106.082420).

Mills S, Alcántara-Rodríguez JA, Ciros-Pérez J, Gómez A, Hagiwara A, Galindo KH, Jersabek CD, Malekzadeh-Viayeh R, Leasi F, Lee J-S, et al. **2017**. Fifteen species in one: deciphering the *Brachionus plicatilis* species complex (Rotifera, Monogononta) through DNA taxonomy. *Hydrobiologia*. 796(1):39–58. doi: [10.1007/s10750-016-2725-7](https://doi.org/10.1007/s10750-016-2725-7).

Moreno E, Pérez-Martínez C, Conde-Porcuna JM. **2019**. Dispersal of rotifers and cladocerans by waterbirds: seasonal changes and hatching success. *Hydrobiologia*. 834(1):145–162. doi: [10.1007/s10750-019-3919-6](https://doi.org/10.1007/s10750-019-3919-6).

Morris JE, Afzelius BA. **1967**. The structure of the shell and outer membranes in encysted *Artemia salina* embryos during cryptobiosis and development. *J Ultrastruct Res*. 20:244–259. doi: [10.1016/S0022-5320\(67\)90285-7](https://doi.org/10.1016/S0022-5320(67)90285-7).

Mundim-Pombo APM, Carvalho HJCD, Rodrigues RR, León M, Maria DA, Migliino MA. **2021**. *Aedes aegypti*: egg morphology and embryonic development. *Parasit Vectors*. 14:1–12. doi: [10.1186/s13071-021-05024-6](https://doi.org/10.1186/s13071-021-05024-6).

Munuswamy N, Hagiwara A, Murugan G, Hirayama K, Dumont HJ. **1996**. Structural differences between the resting eggs of *Brachionus plicatilis* and *Brachionus rotundiformis* (Rotifera, Brachionidae): an electron microscopic study. *Hydrobiologia*. 318(3):219–223. doi: [10.1007/BF00016683](https://doi.org/10.1007/BF00016683).

Nipkow F. **1958**. Beobachtungen bei der Entwicklung des Dauereies von *Brachionus calyciflorus* Pallas. *Schweiz Zeit für Hydrologie*. 20(2):186–194.

Ofem MI, Anyandi AJ, Ene EB. **2017**. Properties of chitin reinforces composites: a review. *Niger J Tech.* 36(1):57–71. doi: [10.4314/njt.v36i1.9](https://doi.org/10.4314/njt.v36i1.9).

Oliver WC, Pharr GM. **2004**. Measurement of hardness and elastic modulus by instrumented indentation: advances in understanding and refinements to methodology. *J Mat Res.* 19(1):3–20. doi: [10.1557/jmr.2004.19.1.3](https://doi.org/10.1557/jmr.2004.19.1.3).

Piavaux A, Magis N. **1970**. Donnees complementaires sur la localisation de la chitine dans les enveloppes des oeufs de Rotifères. *Belgian J Zool.* 100:49–59.

Pourriot R. **1967**. Males et oeufs durables de quelques rotifères. *Bulletin Société Zool France.* 92:85–192.

Pourriot R, Snell TW. **1983**. Resting eggs in rotifers. *Hydrobiologia*. 104:213–224. doi: [10.1007/978-94-009-7287-2_26](https://doi.org/10.1007/978-94-009-7287-2_26).

Rabus M, Sollradl T, Clausen-Schaumann H, Laforsch C. **2013**. Uncovering ultrastructural defences in *Daphnia magna*—an interdisciplinary approach to assess the predator-induced fortification of the carapace. *PLoS One*. 8(6):e67856. doi: [10.1371/journal.pone.0067856](https://doi.org/10.1371/journal.pone.0067856).

Rivas JA Jr, Mohl J, Van Pelt RS, Leung M-Y, Wallace RL, Gill TE, Walsh EJ. **2018**. Evidence for regional aeolian transport of freshwater biota in an arid region. *Limnol Ocean Lett.* 3:320–330. doi: [10.1002/lol2.10072](https://doi.org/10.1002/lol2.10072).

Rivas JA Jr, Schröder T, Gill TE, Wallace RL, Walsh EJ. **2019**. Anemochory of diapausing stages of microinvertebrates in North American drylands. *Freshwater Biol.* 64:1303–1314. doi: [10.1111/fwb.13306](https://doi.org/10.1111/fwb.13306).

Schneider CA, Rasband WS, Eliceiri KW. **2012**. NIH Image to ImageJ: 25 years of image analysis. *Nat Methods*. 9(7):671–675. doi: [10.1038/nmeth.2089](https://doi.org/10.1038/nmeth.2089).

Schröder T. **2005**. Diapause in monogonont rotifers. *Hydrobiologia*. 546:291–306. doi: [10.1007/s10750-005-4235-x](https://doi.org/10.1007/s10750-005-4235-x).

Schröder T, Howard S, Arroyo L, Walsh EJ. **2007**. Sexual reproduction and diapause of *Hexarthra* sp. (Rotifera) in short-lived Chihuahuan Desert ponds. *Freshwater Biol.* 52:1033–1042. doi: [10.1111/j.1365-2427.2007.01751.x](https://doi.org/10.1111/j.1365-2427.2007.01751.x).

Seidman LA, Larsen JH Jr. **1979**. Ultrastructure of the envelopes of resistant and nonresistant *Daphnia* eggs. *Can J Zool.* 57:1773–1777. doi: [10.1139/z79-230](https://doi.org/10.1139/z79-230).

Sellés AG, Marce-Nogué J, Vila B, Perez MA, Gil L, Galobart À, Fortuny J. **2019**. Computational approach to evaluating the strength of eggs: implications for laying in organic egg production. *Biosyst Eng.* 186:46–155. doi: [10.1016/j.biosystemseng.2019.06.017](https://doi.org/10.1016/j.biosystemseng.2019.06.017).

Serra M, Fontaneto D. **2017**. Speciation in the *Brachionus plicatilis* species complex. In: Hagiwara A, Yoshinaga T, editors. *Rotifers fisheries science series*. Singapore: Springer; p. 15–32.

Serra M, Snell TW, King CE. **2004**. The timing of sex in cyclically parthenogenetic rotifers. In: Moya A, Font E, editors. *Evolution from molecules to ecosystems*. Oxford: Oxford University Press; p. 135–146.

Sichlau MH, Hansen JLS, Andersen TJ, Hansen BW. **2010**. Distribution and mortality of diapause eggs from calanoid copepods in relation to sedimentation regimes. *Mar Biol.* 158(3):665–676. doi: [10.1007/s00227-010-1590-6](https://doi.org/10.1007/s00227-010-1590-6).

Ślusarczyk M. **1995**. Predator-induced diapause in *Daphnia*. *Ecology*. 76(3):1008–1013. doi: [10.2307/1939364](https://doi.org/10.2307/1939364).

Snell TW, Burke BE, Messur SD. **1983**. Size and distribution of resting eggs in a natural population of the rotifer *Brachionus plicatilis*. *Gulf Res Rep.* 7(3):285–287. doi: [10.18785/grr.0703.14](https://doi.org/10.18785/grr.0703.14).

Stankiewicz BA, Mastalerz M, Hof CH, Bierstedt A, Flannery MB, Briggs DE, Evershed RP. **1998**. Biodegradation of the chitin-protein complex in crustacean cuticle. *Org Geochem.* 28(1–2):67–76. doi: [10.1016/S0146-6380\(97\)00113-7](https://doi.org/10.1016/S0146-6380(97)00113-7).

Suatoni E, Vicario S, Rice S, Snell TW, Caccone A. 2006. An analysis of species boundaries and biogeographic patterns in a cryptic species complex: the rotifer—*Brachionus plicatilis*. *Mol Phylog Evol.* 41:86–98. doi: [10.1016/j.ympev.2006.04.025](https://doi.org/10.1016/j.ympev.2006.04.025).

Sugumar V, Munuswamy N. 2006. Ultrastructure of cyst shell and underlying membranes of three strains of the brine shrimp *Artemia* (Branchiopoda: Anostraca) from South India. *Microscop Res Tech.* 69(12):957–963. doi: [10.1002/jemt.20371](https://doi.org/10.1002/jemt.20371).

Torres FG, Troncoso OP, Piaggio F, Hijar A. 2010. Structure–property relationships of a biopolymer network: the eggshell membrane. *Acta Biomater.* 6(9):3687–3693. doi: [10.1016/j.actbio.2010.03.014](https://doi.org/10.1016/j.actbio.2010.03.014).

Vargas AL, Santangelo JM, Bozelli RL. 2019. Recovery from drought: viability and hatching patterns of hydrated and desiccated zooplankton resting eggs. *Int Rev Hydrobiol.* 104(1–2):26–33. doi: [10.1002/iroh.201801977](https://doi.org/10.1002/iroh.201801977).

Viitasalo S, Katajisto T, Viitasalo M. 2007. Bioturbation changes the patterns of benthic emergence in zooplankton. *Limnol Ocean.* 52(6):2325–2339. doi: [10.4319/lo.2007.52.6.2325](https://doi.org/10.4319/lo.2007.52.6.2325).

Vinckier A, Semenza G. 1998. Measuring elasticity of biological materials by atomic force microscopy. *FEBS Lett.* 430(1–2):12–16. doi: [10.1016/S0014-5793\(98\)00592-4](https://doi.org/10.1016/S0014-5793(98)00592-4).

Waterkeyn A, Vanoverbeke J, Van Pottelbergh N, Brendonck L. 2011. While they were sleeping: dormant egg predation by *Triops*. *J Plankton Res.* 33(10):1617–1621. doi: [10.1093/plankt/fbr048](https://doi.org/10.1093/plankt/fbr048).

Wurdak E, Gilbert JJ, Jagles R. 1978. Fine structure of the resting eggs of the rotifers *Brachionus calyciflorus* and *Asplanchna sieboldi*. *Trans Am Microscop Soc.* 97(1):49–72. doi: [10.2307/3225684](https://doi.org/10.2307/3225684).

Yin X, Jin W, Zhou Y, Wang P, Zhao W. 2017. Hidden defensive morphology in rotifers: benefits, costs, and fitness consequences. *Sci Rep.* 7(1):4488. doi: [10.1038/s41598-017-04809-z](https://doi.org/10.1038/s41598-017-04809-z).

Zhang C, Wei D, Shi G, Huang X, Cheng P, Liu G, Guo X, Liu L, Wang H, Miao F, et al. 2019. Understanding the regulation of overwintering diapause molecular mechanisms in *Culex pipiens pallens* through comparative proteomics. *Sci Rep.* 9(1):6485. doi: [10.1038/s41598-019-42961-w](https://doi.org/10.1038/s41598-019-42961-w).

Ziv T, Chalifa-Caspi V, Denekamp N, Plaschkes I, Kiersznioska S, Blais I, Admon A, Lubzens E. 2017. Dormancy in embryos: insight from hydrated encysted embryos of an aquatic invertebrate. *Mol Cell Proteomics.* 16:1746–1769. doi: [10.1074/mcp.RA117.000109](https://doi.org/10.1074/mcp.RA117.000109).